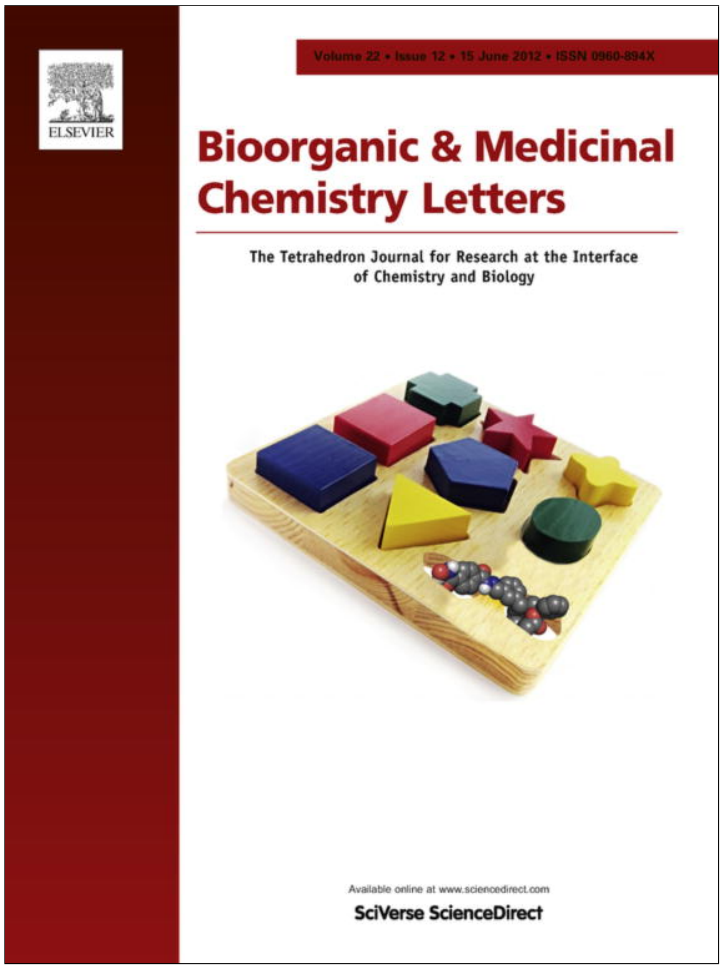

Bioorganic & Medicinal Chemistry Letters 22 (2012) 3998–4003

Contents lists available at SciVerse ScienceDirect

Bioorganic & Medicinal Chemistry Letters

journal homepage: www.elsevier.com/locate/bmcl

Synthesis and evaluation of [^{18}F]Fluorobutyl ethacrynic amide: A potential PET tracer for studying glutathione transferase

Ho-Lien Huang [a,†], Chun-Nan Yeh [b,†], Kang-Wei Chang [c], Jenn-Tzong Chen [c], Kun-Ju Lin [d], Li-Wu Chiang [a], Kee-Ching Jeng [e], Wei-Ting Wang [f], Ken-Hong Lim [f,g], Caleb Gonshen Chen [f,g], Kun-I Lin [a,h], Ying-Cheng Huang [i], Wuu-Jyh Lin [c], Tzu-Chen Yen [d], Chung-Shan Yu [a,j,*]

[a] Department of Biomedical Engineering and Environmental Sciences, National Tsing-Hua University, Hsinchu 300, Taiwan
[b] Department of Surgery, Chang Gung Memorial Hospital at Linkou, Chang Gung University, Taiwan
[c] Institute of Nuclear Energy Research, Taoyuan 32546, Taiwan
[d] Department of Nuclear Medicine, Chang Gung Memorial Hospital at Linkou, Chang Gung University, Taiwan
[e] Taichung Veterans General Hospital, Taichung 40705, Taiwan
[f] Good Clinical Research Center, Department of Medical Research, Mackay Memorial Hospital, Taipei 104, Taiwan
[g] Division of Hematology and Oncology, Department of Internal Medicine, Mackay Memorial Hospital, and Department of Medicine, Mackay Medical College, Taipei 104, Taiwan
[h] Departments of Obstetrics & Gynecology, Chang Bing Show Chwan Memorial Hospital, Lukang Zhen, Changhua County, Taiwan
[i] Department of Neurosurgery, Chang Gung Memorial Hospital at Linkou, Chang Gung University, Taiwan
[j] Institute of Nuclear Engineering and Science, National Tsing-Hua University, Hsinchu 300, Taiwan

ARTICLE INFO

Article history:
Received 22 February 2012
Revised 3 April 2012
Accepted 19 April 2012
Available online 30 April 2012

Keywords:
Imaging
GST-α
Cholangiocarcinoma
Tumor
Cold spot

ABSTRACT

[^{18}F]Flurobutyl ethacrynic amide ([^{18}F]FBuEA) was prepared from the precursor tosylate *N*-Boc-*N*-[4-(toluenesulfonyloxy)butyl]ethacrynic amide with a radiochemical yield of 3%, a specific activity of 48 GBq/μmol and radiochemical purity of 98%. Chemical conjugation of [^{18}F]FBuEA with glutathione (GSH) via a self-coupling reaction and enzymatic conjugation under catalysis of glutathiontransferase alpha (GST-α) and π provided about 41% yields of radiochemical conjugated product [^{18}F]FBuEA–GSH, 85% and 5–16%, respectively. The catalytic selectivity of this tracer toward GST-alpha was addressed. Positron emission tomography (PET) imaging of [^{18}F]FBuEA in normal rats showed that a homogeneous pattern of radioactivity was distributed in the liver, suggesting a catalytic role of GST. By contrast, PET images of [^{18}F]FBuEA in rats with thioacetamide-induced cholangiocarcinoma displayed a heterogeneous pattern of radioactive accumulation with cold spots in tumor lesions. PET imaging with [^{18}F]FBuEA could be used for early diagnosis of hepatic tumor with a low GST activity as well as liver function.

Glutathion transferase (GST) represents a major group of detoxification enzymes.[1] All eukaryotic species possess multiple cytosolic and membrane bound GST isoenzymes, each of which displays distinct catalytic as well as noncatalytic binding properties. The cytosolic enzymes are encoded by seven distantly related gene families (designated class alpha, pi, mu, theta, omega, zeta, and sigma). The most abundant mammalian GSTs are the class alpha, mu, and pi enzymes. The biological control of these enzymes is complicated as they exhibited sex-, age-, tissue-, species-, and tumor-specific patterns of expression. GSTs are regulated by structurally diverse xenobiotics. Many inducers can further affect transcriptional activation of GST genes, for example, antioxidant responsive element (ARE) and the xenobiotic-responsive element (XRE). In addition, compounds that induce GST are themselves substrates for these enzymes, or are metabolized to compounds that can serve as GST substrates. The majority of human tumors and human tumor cell lines expressed significant amounts of pi GST. The human alpha class GSTs consist of 5 genes, *hGSTA1–hGSTA5*. The homodimer hGSTA1-1 (and to a lesser extent hGSTA2-2)[2] catalyzes the GSH-dependent detoxification of carcinogenic metabolites of environmental pollutants, tobacco smoke, and several alkylating chemotherapeutic agents. hGSTA1-1 and hGSTA2-2 are expressed at high levels in liver, intestine, kidney, adrenal gland, and testis. Alpha class GSTs have been suggested to be involved in susceptibility to diseases with environmental causes (such as cancer, asthma, and cardiovascular disease) and in response to chemotherapy. Although hGSTM1, hGSTT1, and hGSTP1 have been associated with such diseases, alpha class GSTs has not been well studied in this respect and its molecular basis for the variation is less clear.

Abbreviations: *CCA*, cholangiocarcinoma; *TAA*, thioacetamide; *NERI*, Nuclear Energy Research Institute; *CGMH*, Chang-Gung Memorial Hospital.

* Corresponding author.
E-mail address: csyu@mx.nthu.edu.tw (C.-S. Yu).

† These authors contributed equally to this work.

0960-894X/$ - see front matter © 2012 Elsevier Ltd. All rights reserved.
http://dx.doi.org/10.1016/j.bmcl.2012.04.091

Cholangiocarcinoma (CCA) is a cancer derived from bile duct epithelium (i.e. cholangiocytes). It is characterized by a great diversity of symptoms commonly occurring in the late course of the disease, and therefore making treatment difficult.[3] CCA is related to a wide range of risk factors, such as infestation with liver flukes, primary sclerosing cholangitis, and hepatolithiasis, liver cirrhosis and causes various incidence rates of CCA in different areas of the world.[4] However, data have shown that the incidence and mortality rates of CCA have been rising worldwide over past decades, particularly the intrahepatic CCA.[5–7] An oral thioacetamide (TAA)-induced model of rat CCA has been used to study the therapeutics responses with tumor measurement and molecular imaging using 2-deoxy-2-[^{18}F]fluoroglucose (FDG) with positron emission tomography (PET).[8] The average PET signal of tumor to liver ratio was 1.60. Given the fact that all the human, rat and mice contain 5 subclasses of GSTα and one subclass of GSTπ (two GSTπ isoforms in mice), an animal model of TAA-induced CCA would be the choice for developing potential compounds for studying the liver function.

There are two criteria of an ideal probe for studying the potential marker GSTπ:[9,10] firstly it should be a good substrate to be conjugated with glutathione (GSH) under catalysis of GSTπ. Secondly, the molecule should be tagged with appropriate moieties and thus it can be traceable by detecting the emitting photons which are energetically enough to penetrate the animal tissues. A number of compounds showed marked differential affinities toward GST isoenzymes-catalyzed conjugation with GSH; for example, $\triangle^5$ androstene-3,17-dione, selective for rGSTA1 and/or A2 subunits; 4-hydroxynonenal, selective for rGSTA4; 1,2-dicholoro-4-nitrobenzene (DCNB), selective for rGSTM1.[1] 1-Choloro-2,4-dinitrobezene (CDNB) and ethacrynic acid (EA) are classified as the relatively nonselective substrates. CDNB shows broad affinities toward almost all GST isoenzymes. By contrast, EA shows a moderate substrate affinity toward rGSTP1-1. Hence, the recent report of a butyl ethacrynic amide,[11–13] a butyl analog of EA, which showed a modified cytotoxicity against tumor cells, attracts our attention (Fig. 1).[14]

Regarding the second criterion, the substrate should be tagged with a photon emitter with a size small enough to not to hamper its original biological activity. Positron emitters, for example, ^{18}F emitting two energetic photons (511 keV) in an angle of 180° has been coupled with PET for a wide use in diagnostic medicine.[15,16] The characteristics of ^{18}F, such as low radiation doses, short tissue range, feasibility of multistep synthesis and extendable scanning protocols are attributed to a relatively low energy of 0.64 MeV and a relatively long half-life ($t_{1/2}$ = 109.7 min). The adequate atomic size due to being a member of the second periodic atoms makes ^{18}F a suitable atom for mimicking oxygen or hydrogen. The high sensitivity of ^{18}F allows the use of a very low concentration (10^{-12} M) of radiolabeled tracer for imaging cellular markers, for example, receptors without encountering toxicity concerns. Introduction of ^{18}F can be mediated through a direct substitution reaction or an indirect reaction via a bifunctional group.[17,18] The former includes a nucleophilc or electrophilic pathway. Taken together, we attempt to prepare ^{18}F-labeled FBuEA analog **3** as a substrate to assess its potential use as an in vivo imaging agent for studying GST isoenzymes in CCA rats. The structure of FBuEA **3** showed that fluorine at the end position of the butyl group should not alter the enone functionality. In addition, the precursor for radiofluorination is a primary alcohol-derived tosylate, which has been widely used for radiofluorination in radiochemistry.

Preparation of precursor (8). The preparation of the desired alcohol **12** was initially started from a methyl ester of EA, which was prepared by using CH_2N_2 and EA (Scheme 1 of Supplementary data). Whereas the ester could be obtained in satisfactory yield (70%), subsequent coupling with the unprotected 4-aminobutyl alcohol provided the desired amide coupling product in only 20% yield due to the lack of regioselectivity and the less reactive ester (Scheme 1 of Supplementary data). Hence, by adopting the usual HBTU-mediated amide coupling protocol in association with the source carboxylic acid **2** and the well-protected *O*-TBDMS butyl amine **4**,[19] a satisfactory yield of 70% of amide **5** was obtained (Scheme 1). Recently, the preparation of 3-hydroxypropyl ethacrynic amide has been prepared from EA acyl chloride without protecting the hydroxy group.[20]

Prior to the next step, the synthetic strategy was examined. When the tosyl group is substitutable by [^{18}F]fluoride ion from tetrabutyl ammonium fluoride, the imido proton of the tautomer could be removed by the basic fluoride and resulted in a good nucleophilic state readily for intramolecular cyclization. The anticipitated ring closure that forms a 7-membered ring might reduce the radiochemical yield, because we observed in a similar case with 5-membered ring formation when performing a fluorination for 5-(2-tolylsulfonylethyl)-2′-deoxyuridine analog.[21] Therefore, an adequate protection at the amide group is needed.

An attempt to protect the amide group with acetyl group using isoproprenyl acetate failed to provide the *N*-acetyl product **5** and produced only the undesired *O*-acetyl byproduct, probably due to the instability of the silyl group (Scheme 2 of Supplementary data). Hence, through an alternative treatment with $(Boc)_2O$, the desired Boc-protected product **6** could be obtained in 76% yield. By removing the silyl group with the combination of tetrabutyl ammonium fluoride (TBAF) and AcOH, the desired product **7** could be obtained in quantitative yield. However, in a parallel experiment under the presence of 4 Å MS, the cyclized hemiacetal byproduct **14** was solely obtained in 30% yield (Scheme 3 of Supplementary data). With the alcohol **7** prepared, either the subsequent fluorination with DAST to provide the nonradioactive compound **9** or the preparation of tosylate **8** using TsCl can be performed. The cold compound **9** and cold FBuEA **3** were both used as authentic

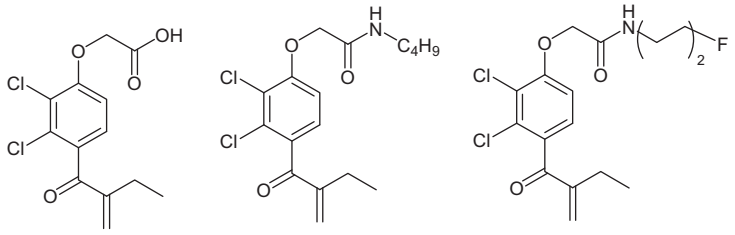

1 Ethacrynic acid — IC_{50} = 84 μM

2 BuEA — IC_{50} = 13 μM

3 FBuEA — IC_{50} = 8 μM[14]

Figure 1. Cytotoxicities of ethacrynic acid analogs against A549 cells.

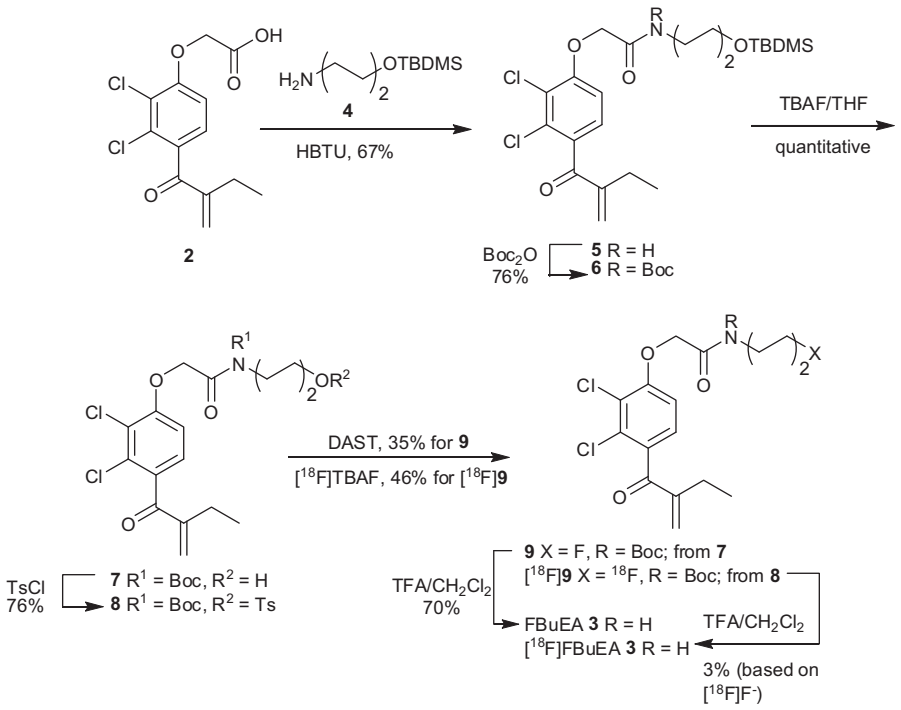

Scheme 1. Synthesis of nonradioactive compound **9** and deprotected FBuEA **3** as authentic samples for radiochemical synthesis of [^{18}F]**9** and [^{18}F]FBuEA **3**.

samples throughout the radiochemical synthesis for optimizing the radiochemical yield.

In order to obtain a satisfactory radiochemical yield from radiofluorination, it is critical to have sufficiently pure tosylate **8.** Therefore, **s**amples were collected from centered fractionations of column chromatography with a number of tosylate **8** preparations and the purity was met with criteria by elemental analysis.

Radiosynthesis of [^{18}F]FBuEA 3. The preparation was carried out by using the tosylate **8** (10 mg) and [^{18}F]$F^-N^+Bu_4$. [^{18}F]**9** was obtained in an average radiochemical yield of 46%. The subsequent removal of the Boc group using trifluoro acetic acid (TFA) at ambient temperature was accomplished in 7% yield, whereas a more rigorous condition of using 50 °C in association with reduced equivalents of TFA did not produce the desired [^{18}F]FBuEA **3**. The HPLC chromatogram of the product mixture using a normal phase column showed an UV active peak at t_R = 8.5 min, suggesting the released leaving group [Fig. 2(A)]. Whereas this UV active substance and the nonpolar radioactive unknown substance (t_R = 5.0 min) may not disturb the PET imaging outcomes of [^{18}F]FBuEA **3**, additional purification with semi-preparative HPLC was used, and the isolated fractions obtained reached a radiochemical purity of 98% and specific activity of greater than 48 GBq/μmol [Fig. 2(B)].

Interestingly, hydrolyzed byproduct or the byproduct from elimination was not observed in the chromatogram either before or after HPLC purification, which might be attributed to the previous manipulation of the cartridge settings. The present protocol for preparing [^{18}F]FBuEA **3** (ready for tail vein injection), which involved the two-step radiochemical synthesis including deprotection, collection of the fractions isolated from HPLC and concentration under reduced pressure was accomplished with a radiochemical yield of 2.3% (decay corrected) within 1.5 h (end of bombardment, EOB).

Radiosynthesis of [^{18}F]FBuEA–GSH (10). The radiochemical yield (41%) of [^{18}F]**10** obtained from selfconjugation of [^{18}F]FBuEA **3** with GSH under pH 8.0[22] is less than the yield that reported previously.[23,24] In contrast to the radio TLC estimation reported by these literatures, the current yield calculation was based on the isolated product from HPLC purification. On the other hand, the nonradioactive authentic sample FBuEA–GSH **10** was prepared under the same reaction condition (see Supplementary data) and the yield was slightly greater than 41%. The two diastereomers were

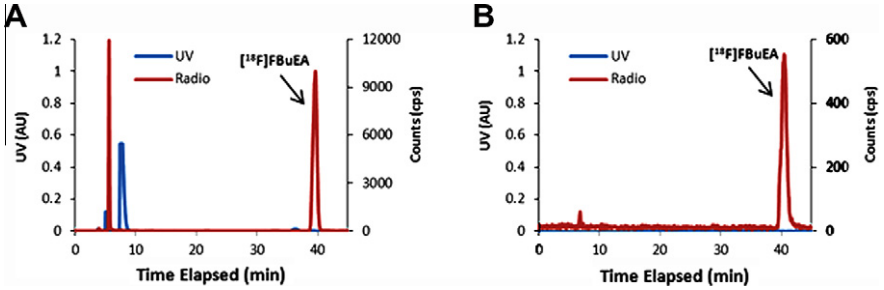

Figure 2. Chromatogram for [^{18}F]FBuEA before (A) and after (B) HPLC purification. A normal phase semipreparative column (Si-100) was employed. AU: Arbitrary Unit. Eluting condition: [(A), see Supplementary data], CPS: counts per second.

observed from ^{1}H NMR in a ratio of 3:2. A further separation using chiral column will be carried out in future study.

Conjugation of [^{18}F]FBuEA (3) with GST under catalysis of GST-π and GST-α. The method reported by Lo et al.[25] was adopted to perform this conjugation (Scheme 2). In their work, a prolonged reaction time (2 h) could assure that the reaction achieved completion. The conjugating experiment using [^{18}F]FBuEA **3** and GSH under catalysis by GST-π gave [^{18}F]FBuEA–GSH **10** in 16% yield (5% from another assay). By contrast, a high conversion yield of 85% was observed in the case of GST-α (Fig. 3B). The selectivity of [^{18}F]FBuEA **3** toward GST-α may allow the study of the functions of liver since it constitutes the major portion of GST enzyme in liver. The present findings are different from our initial aim for targeting GST-π and now it is clear that the application of [^{18}F]FBuEA **3** should be confined to the study of liver function. An appropriate liver disease model is needed therefore. The recently reported CCA rat with liver tumors induced by TAA emerges as the suitable animal model for the preliminary assessment of the probe.

Metabolite analysis. Before carrying out the animal imaging experiment, the stability of [^{18}F]FBuEA **3** in vivo was assessed by HPLC measurement of the radioactivity remaining in the blood.[26,27] As shown in Figure 4, the in vivo half-life of [^{18}F]FBuEA **3** was determined to be 46 min ($t_{1/2}$). Compared to the plasma half-life of 0.5–1 h of the parent ethacrynic acid,[28] the hydrophobic butyl moieties of [^{18}F]FBuEA **3** did not significantly alter the duration time.

Small Animal PET imaging of [^{18}F]FBuEA (3). Figure 5 shows small animal PET images averaged from 0 to 120 min timeframes postinjection of [^{18}F]FBuEA **3**. After intravenous application of [^{18}F]FBuEA **3**, the radiotracer was rapidly distributed. The liver is the main site of accumulation of [^{18}F]FBuEA **3**, which could be explained by the formation of the [^{18}F]FBuEA–GSH **10** complex as well as its subsequent transformation by membrane transporters. Due to the size limitation of the MicroPET scanner of NERI, only local imaging could be studied on the rat. However, when mouse was investigated, a whole-body image was obtained and a rapid radioactivity distribution was reached as early as the first 5 min in several organs including liver, kidney and bladder (data not shown). Although [^{18}F]FBuEA **3** was initially assumed to be capable of intracellular accumulation in tumors, a vast abundance of GSH and the presence of GST especially GST-α in liver could overwhelmingly dominate the formation of [^{18}F]FBuEA–GSH **10** complexes. The accumulation of [^{18}F]FBuEA **3** was homogeneously distributed over the liver of the normal rat [Fig. 5(A)]. By contrast, a heterogeneous distribution of [^{18}F]FBuEA **3** in the liver of the CCA rat was noted [Fig. 5(B)]. The cold spots with no radioactivity accumulation suggested a low level of GST. The two rats were then sacrificed and their photographs [Fig. 5(C and D)] showed significantly pathological differences. The initial assessment of [^{18}F]FBuEA showed a negative correlation between GST isoenzymes and the tumor progression of the infiltrative liver of CCA rat.

Being a promising imaging probe, [^{18}F]FBuEA **3** should be capable of detecting a disease at its early stage. Since an oversaturation of the imaging signal of normal rat was observed with a timeframe averaging from 0 to 120 min [Fig. 5(A)], a shorter imaging

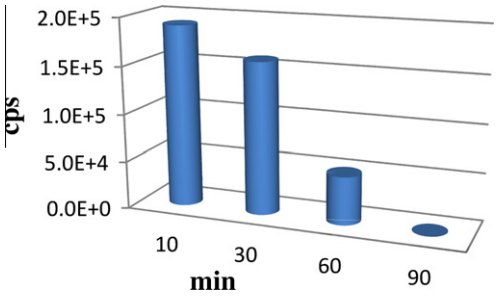

Figure 4. Metabolite analysis of [^{18}F]FBuEA **3**. Time-activity relationship obtained by integrating the counts of the peak corresponding to [^{18}F]FBuEA **3** from the chromatogram taken at each time point. Plasma $T_{1/2}$ = 46 min. CPS: counts per second.

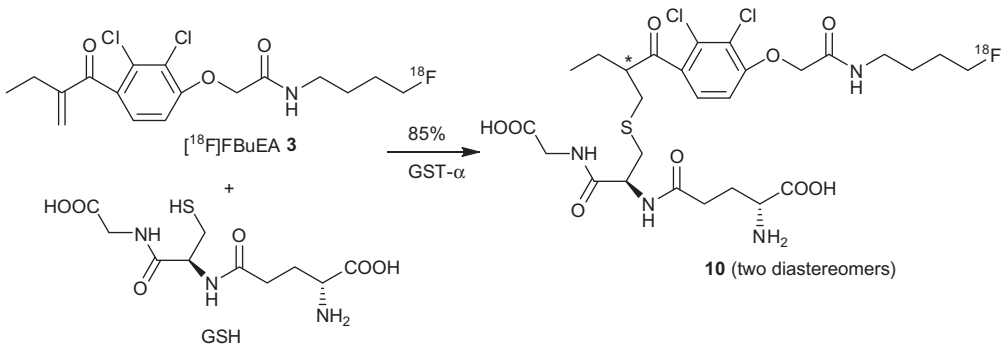

Scheme 2. Formation of the [^{18}F]FBuEA–GSH **10** complex under the catalysis of GST-α.

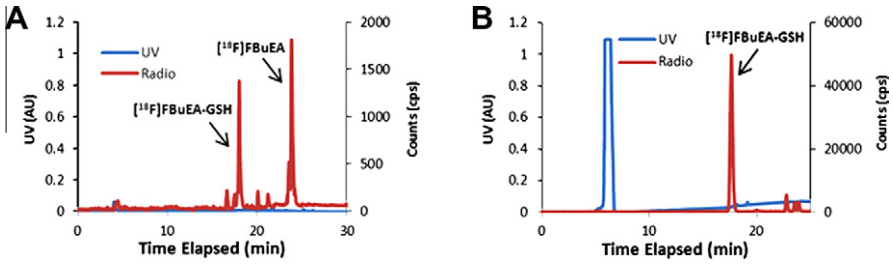

Figure 3. RP-HPLC chromatogram of the mixtures of [^{18}F]FBuEA–GSH (t_R = 17.5 min) and the residual [^{18}F]FBuEA (t_R = 23.7 min) obtained from selfconjugation under pH 8 [Fig. 3(A)] and under catalysis of GST-α [Fig. 3(B)]. The peak at t_R = 5.8 min was suggested to be GST-α.

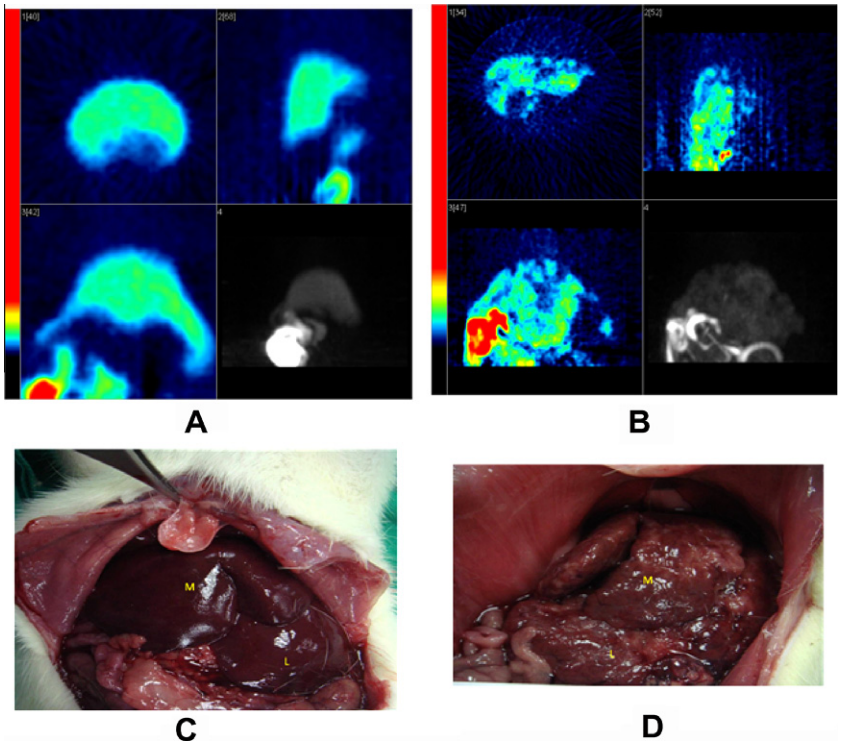

Figure 5. (A) PET images of the normal rat were normalized from 0 to 120 min post injection. Injection dose: 717 μCi/1 mL. The frames are composed of four subframes which were denoted individually by upper left subframe: transverse cross section, upper right subframe: sagittal cross section, lower left subframe: coronal cross section, and lower right subframe: coronal cross section with contrast. (B) PET images of the rat of CCA (feeding with TAA for 24 weeks) were normalized from 0 to 120 min post injection. Injection dose: 569 μCi/0.6 mL. The two rats were then sacrificed and photographs were taken for both (C) and the CCA rat (D). Labels: M and L denote middle liver and left liver, respectively.

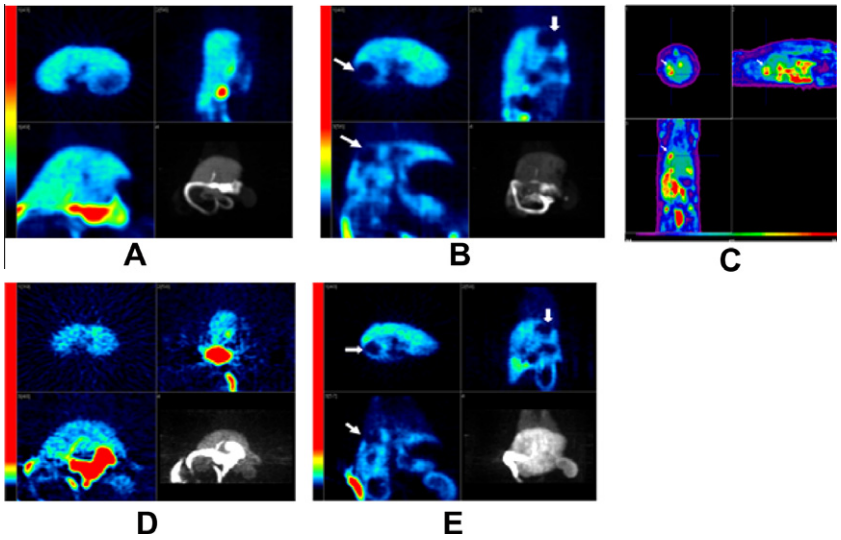

Figure 6. (A) PET images of the normal rat using [^{18}F]FBuEA were average of dynamic images of time frame from 0 to 30 min. Injection dose: 265 uCi/0.25 mL. (B) PET images of the CCA rat (feeding with TAA for 18 weeks) using [^{18}F]FBuEA were average of dynamic images of time frame from 0 to 30 min post injection. Injection dose: 486 μCi/0.23 mL. Arrow indicates the lesion of tumor. (C) PET images of the same CCA rat as that of (B) were taken by using [^{18}F]FDG post 90 min. Arrow indicates the lesion of tumor. This PET image was carried out in Chang-Gung Memorial Hospital. (D) PET images of the normal rat were average of dynamic images of time frame from 5 to 10 min post injection. Injection dose: 764 μCi/0.8 mL. (E) PET images of the same rat as that described in (B) with a prolonged feeding to 23 weeks of TAA were average of dynamic images of time frame from 5 to 10 min post injection. Injection dose: 801 μCi/0.5 mL.

time frame was adopted. As shown in Figure 6(C), PET images of CCA-rat receiving TAA for 18 weeks using [^{18}F]fluorodeoxyglucose ([^{18}F]FDG) indicated a significant hot spot implying a tumor lesion. Then the CCA rat along with the normal rat were subsequently imaged with [^{18}F]FBuEA **3** 5 days later. As shown in Figure 6(B), the same region of the CCA rat that highlighted by [^{18}F]FDG showed a cold spot instead and with a more diffused signal pattern that suggested either a deficiency in GST-α expression or an extraordinary function of GST. The same CCA rat after feeding for 23 weeks of TAA was imaged again with [^{18}F]FBuEA **3** but the imaging time

was shortened to 5–10 min for optimization test [Fig. 6(D and E)]. Whereas the tumor lesion was still dark and the cold spot was similar to that of 18 week rat. From the above comparisons, the optimized imaging sampling times appears to be 0–30 min. These results suggest that regulation of GST-α synthesis was disturbed. A work reported by Ling et al. has addressed a similar finding of decreased synthesis of GST-α during the process of hepatocarcinogenesis.[29] Although the cytotoxicity of the nonradioactive FBuEA **3** against A549 might imply its preferential accumulation in tumors through GST catalysis and the corresponding radioactive [^{18}F]FBuEA **3** displaced a hot spot, another cytotoxic mechanism via Wnt signaling pathway could also be involved.[20] The level of expression of GST, specifically GST-α, might be negatively correlated to that of Wnt signaling proteins.

Whereas the current cold spot prevents its use from tracing the metastasis to other organs, [^{18}F]FBuEA **3** might be capable of assessing the liver function based on GST activity. For example, the clinical efficacy of current chemotherapeutic drugs, for example, mephalan and temozolomide by exerting their cytotoxicities via alkylation mechanism is inevitably retarded by GST of the liver. Liver cancer or other types of cancers with low GST activity might be suitable for treatment with this type of drugs.

In brief, the radiolabeled compound [^{18}F]FBuEA **3** was prepared based on an initial cellular-based screening of a library of ethacrynic acid-derived amide formation products using solution phase parallel synthesis.[30] [^{18}F]FBuEA **3** was prepared via the nucleophilic radiofluorination of the precursor tosylate **8**, from ethacrynic acid via a 4-step synthesis. A sufficient radiochemical yield of 3% and specific activity of 48 GBq/μmol was obtained from these procedures. The liver is the major organ for the tracer uptake, and glutathione and GST enzymes play a role in the metabolism of this tracer. An in vivo half-life of 46 min for [^{18}F]FBuEA **3** obtained from a preliminary in vivo stability test for [^{18}F]FBuEA **3** is shorter than the half-life of ^{18}F. The adequate clearance rate is capable of providing an acceptable contrasting image for the TAA-treated CCA rat. [^{18}F]FBuEA **3** was found to be accumulated homogeneously in the liver of normal rat using PET. However, an extraordinary change in the liver image was observed in the CCA rat at the early stage of tumor development and suggested its diagnostic potential.

Acknowledgments

We are grateful to the National Science Council of Taiwan, CGMH_NTHU Joint Research and Chang-Gung Medical Research Project for providing financial support of the Grant numbers of NSC-98-2113-M-007-012, NSC-97-2314-B-182A-020-MY3, CGTH9 6N2342E1, CMRPG390931, CMRPG391512 and CMRPG3B0361. Technical assistance by Mr. Yean-Hung Tu and Ms. Li-Yuan Huang are acknowledged. We acknowledge Dr. Shui-Tein Chen from Institute of Biological Chemistry at Academia Sinica for his review of this manuscript.

Supplementary data

Supplementary data associated with this article can be found, in the online version, at http://dx.doi.org/10.1016/j.bmcl.2012.04.091.

References and notes

1. Hayes, J. D.; Pulfor, D. J. *Crit. Rev. Biochem. Mol. Biol.* **1995**, *30*(6), 445.
2. Sies, H.; Packer, L. Human alpha class glutathione *S*-transferase genetic polymorphism, expression, and susceptibility to disease In *Methods in Enzymology*; Coles, B. F., Kadlubar, F. F., Eds.; Elsevier Academic Press: San Diego, USA, 2005; Vol. 41, p 9.
3. Liver Cancer Study Group of Japan. Classification of primary liver cancer. 1st English ed. Tokyo: Kanehara Shuppan, 1997.
4. Shaib, Y.; El-Serag, H. B. *Semin. Liver Dis.* **2004**, *24*, 115.
5. Shaib, Y. H.; Davila, J. A.; McGlynn, K.; El-Serag, H. B. *J. Hepatol.* **2004**, *40*, 472.
6. Patel, T. *BMC Cancer* **2002**, *2*, 10.
7. Chang, K. Y.; Chang, J. Y.; Yen, Y. *J. Natl. Compr. Canc. Netw.* **2009**, *7*, 423.
8. Yeh, C. N.; Lin, K. J.; Hsiao, I. T.; Yen, T. C.; Chen, T. W.; Jan, Y. Y.; Chung, Y. H.; Lin, C. F.; Chen, M. F. *Mol. Imaging Biol.* **2008**, *10*, 209.
9. Townsend, D. M.; Tew, K. D. *Oncogene* **2003**, *22*, 7369.
10. McIlwain, C. C.; Townsend, D. M.; Tew, K. D. *Oncogene* **2006**, *25*, 1639.
11. Chiang, L.-W.; Pei, K.; Chen, S.-W.; Huang, H.-L.; Lin, K.-J.; Yen, T.-C.; Yu, C.-S. *Chem. Pharm. Bull.* **2009**, *57*, 714.
12. Wang, K.; Li, C.; Song, D.; Zhao, G.; Zhao, L.; Jing, Y. *Cancer Res.* **2007**, *67*, 7856.
13. Su, Y. H.; Chiang, L. W.; Jeng, K.-C.; Huang, H.-L.; Chen, J.-T.; Lin, W.-J.; Huang, C.-W.; Yu, C.-S. *Bioorg. Med. Chem. Lett.* **2011**, *21*, 1320.
14. *Unpublished results.* IC_{50} of FBuEA against MCF7 and A549 were 3 and 8 μM, respectively. A parallel assay: IC_{50} of FBuEA against A549 and IMR-90 (fibroblast as a control) were 21 and 18 μM, respectively. IC_{50} of BuEA against MCF7 and A549 were 4 and 13 μM, respectively.
15. Miller, P. W.; Long, N. J.; Vilar, R.; Gee, A. D. *Angew. Chem., Int. Ed.* **2008**, *47*, 8998.
16. Li, Z.; Conti, P. S. *Adv. Drug Delivery Rev.* **2010**, *62*, 1031.
17. Tolmachev, V.; Stone-Elander, S. *Biochim. Biophys. Acta-Gen. Subj.* **2010**, *1800*, 487.
18. Lee, S.; Xie, J.; Chen, X. *Chem. Rev.* **2010**, *110*, 3087.
19. Krivickas, S. J.; Tamanini, E.; Todd, M. H.; Watkinson, M. *J. Org. Chem.* **2007**, *72*, 8280.
20. Jin, G.; Lu, D.; Yao, S.; Wu, C. C. N.; Liu, J. X.; Carson, D. A.; Cottam, H. B. *Bioorg. Med. Chem. Lett.* **2009**, *19*, 606.
21. Yu, C.-S.; Oberdorfer, F. *Synthesis* **1999**, 2057.
22. Shi, B. L.; Stevenson, R.; Campopiano, D. J.; Greaney, M. F. *J. Am. Chem. Soc.* **2006**, *128*, 8459.
23. Berndt, M.; Pietzsch, J.; Wuest, F. *Nucl. Med. Biol.* **2007**, *34*, 5.
24. Wuest, F.; Hultsch, C.; Bergmann, R.; Johannsen, B.; Henle, T. *Appl. Rad. Isot.* **2003**, *59*, 43.
25. Lo, W.-J.; Chiou, Y.-C.; Hsu, Y.-T.; Lam, W.-S.; Chang, M.-Y.; Jao, S.-C.; Li, W.-S. *Bioconjugate Chem.* **2007**, *18*, 109.
26. Tracqui, A.; Kintz, P.; Mangin, P. Systematic toxicological analysis using HPLC/DAD. In *HPLC method for pharmaceutical analysis*; George, L., Norman, S., Eds.; Wiley-Interscience Press: New York, USA, 1997; p 35.
27. Uddin, M. J.; Crews, B. C.; Blobaum, A. L.; Kingsley, P. J.; Gorden, D. L.; McIntyre, J. O.; Matrisian, L. M.; Subbaramaiah, K.; Dannenberg, A. J.; Piston, D. W.; Marnett, L. J. *Cancer Res.* **2010**, *70*, 3618.
28. Hardman, J. G.; Goodman, G. A.; Limbird, L. E. In *Goodman and Gilman's The pharmacological basis of therapeutics*, 9th ed.; McGraw-Hill Companies: Southern California, 1996.
29. Ling, L.; Higashi, T.; Tsuchida, S.; Sato, K.; Tsuji, T. *Acta Med. Okayama* **1993**, *47*, 293.
30. Boger, D. L.; Desharnais, J.; Capps, K. *Angew. Chem., Int. Ed.* **2003**, *42*, 4138.